# Bio-Trapping Ureolytic Bacteria on Sand to Improve the Efficiency of Biocementation

Gizem Elif Ugur<sup>1</sup>, Kylee Rux<sup>2</sup>, John Connor Boone<sup>1</sup>, Rachel Seaman<sup>3</sup>, Recep Avci<sup>4</sup>, Robin Gerlach<sup>3,5</sup> Adrienne Phillips<sup>2,3</sup>, Chelsea Heveran<sup>1,3#</sup>

**Keywords:** biocementation, *Sporosarcina pasteurii*, microbial induced calcium carbonate precipitation (MICP), bio-trapping, aminosilane functionalization

<sup>&</sup>lt;sup>1</sup> Mechanical and Industrial Engineering Department, Montana State University, Bozeman, MT 59717, USA

<sup>&</sup>lt;sup>2</sup> Civil and Environmental Engineering Department, Montana State University, Bozeman, MT 59717, USA.

<sup>&</sup>lt;sup>3</sup> Center for Biofilm Engineering, Montana State University, Bozeman, MT 59717, USA

<sup>&</sup>lt;sup>4</sup> Department of Physics, Montana State University, Bozeman, MT 59717, USA

<sup>&</sup>lt;sup>5</sup> Chemical & Biological Engineering Department, Montana State University, Bozeman, MT 59717, USA #Corresponding author: <a href="mailto:chelsea.heveran@montana.edu">chelsea.heveran@montana.edu</a>

#### Abstract

Microbially induced calcium carbonate precipitation (MICP) has emerged as a novel technology with the potential to produce building materials through lower-temperature processes. The formation of calcium carbonate bridges in MICP allows the biocementation of aggregate particles to produce bio-bricks. Current approaches require several pulses of microbes and mineralization media to increase the quantity of calcium carbonate minerals and improve the strength of the material, thus leading to a reduction in sustainability. One potential technique to improve the efficiency of strength development involves trapping the bacteria on the aggregate surfaces using silane coupling agents, such as positively charged 3aminopropyl-methyl-diethoxysilane (APMDES). This treatment traps bacteria on sand through electrostatic interactions that attract negatively charged walls of bacteria to positively charged amine groups. The APMDES treatment promoted abundant and immediate association of bacteria with sand, increasing the spatial density of ureolytic microbes on sand and promoting efficient initial calcium carbonate precipitation. Though microbial viability was compromised by treatment, urea hydrolysis was minimally affected. Strength was gained much more rapidly for APMDES-treated sand than for untreated sand. Three injections of bacteria and biomineralization media using APMDES-treated sand led to the same strength gain as seven injections using untreated sand. The higher strength with APMDES treatment was not explained by increased calcium carbonate accrual in the structure and may be influenced by additional factors, such as differences in the microstructure of calcium carbonate bridges between sand particles. Overall, incorporating pre-treatment methods, such as amine silane coupling agents, opens a new avenue in biomineralization research by producing materials with improved efficiency and sustainability.

#### 1. Introduction

The demand for infrastructure materials is continuously increasing. The impact of this high demand for concrete is that cement, the binding component of concrete, is the second most consumed resource in the world after water <sup>1</sup>. The production of ordinary portland cement is responsible for generating 5-8% of global anthropogenic greenhouse gas emissions <sup>2</sup>. Alternative methods of manufacturing construction materials with greater sustainability are needed. Microbially induced calcium carbonate precipitation (MICP) has been the subject of considerable research interest for its potential to strengthen soils, seal cracks, and generate building materials through lower temperature processes <sup>3–8</sup>. The enzyme urease produced by ureolytic bacteria, such as *Sporosarcina pasteurii* (*S. pasteurii*), catalyzes urea hydrolysis to produce ammonium (NH<sub>4</sub><sup>+</sup>) and carbonate ions (CO<sub>3</sub><sup>2–</sup>). In the presence of (Ca<sup>2+</sup>), the reaction becomes favorable for CaCO<sub>3</sub> precipitation (Equations 1-2).

$$CO(NH2)2 + H2O \xrightarrow{Urease} 2NH4^+ + CO32-$$
 (1)

$$Ca^{2+} + CO_3^{2-} \longrightarrow CaCO_3 \tag{2}$$

Strength development through MICP relies on establishing calcium carbonate bridges between aggregate particles, which serves to biocement the material <sup>6,8–10</sup>. It is well-established that strength can be increased by increasing the quantity of calcium carbonate within the material, which is achieved through repeated injections of microbes and biocementation medium or higher concentrations of reactants <sup>9–12</sup>. Therefore, strength gain is usually achieved at the expense of sustainability <sup>3,13,14</sup>. Since the MICP reaction occurs in the immediate proximity of the bacteria, controlling the location of bacteria could provide a new approach for improving the efficiency of strength development.

Attempts to control bacterial spatial distribution for biocementation have been limited. One strategy was to adjust the salinity of the bacterial suspension or injecting soil with saline solution to improve the retention of bacteria. However, this has important disadvantages, such as exposing bacteria to osmotic shock, thus potentially compromising microbial viability or activity, or increasing the risk for corrosion <sup>15</sup>. Another potential method to improve spatial control over MICP is to trap the bacteria on the

aggregate surfaces using silane coupling agents. An example of this technology is BiyoTrap <sup>16</sup> which functionalizes surfaces with 3-aminopropyl-methyl-diethoxysilane (APMDES). The chemical modification covalently attaches positively charged amine groups onto surfaces, on which have hydroxyl groups, thus electrostatically attracting negatively charged walls of bacteria <sup>16–19</sup>. Silica sand already has hydroxyl moieties on its surface <sup>20</sup>, but the spatial density of these groups can be increased through ozone treatment. After APMDES treatment, bacteria are localized to the charged area but are not strictly immobilized <sup>16</sup>. APMDES and similar treatments have been utilized to rapidly detect trace amounts of bacteria in liquids such as drinking water sources and contaminated liquids, as well as to isolate sulfate-reducing bacteria <sup>16,21,22</sup>. Various surfaces have been successfully functionalized to bio-trap bacteria, including silicon, glass, and glass wool fibers <sup>16,22–24</sup>. However, APMDES treatment has not yet been explored as a method to functionalize aggregates for the purpose of spatially controlling bacteria to achieve biocementation. The purpose of this study was to test the hypothesis that trapping bacteria on sand surfaces treated with APMDES would increase the efficiency of strength development during biocementation.

## 2. Materials and Methods

#### 2.1 Materials

## 2.1.1 Sand

Quikrete™ Commercial Medium Sand (#196251) was used in all the experiments. Sand was soaked in a 4% HCl solution overnight to remove metal contaminants. Afterward, the pH was balanced to 7 by adding sodium bicarbonate, before the sand was rinsed with tap water and left to air-dry at room temperature. After drying, the sand was sterilized by autoclaving at 121 °C for 1 h.

#### 2.1.2 Growth and biocementation media

The growth medium used for the starter culture contained 37 g L<sup>-1</sup> Brain Heart Infusion (BHI) (Becton Dickinson, Franklin Lakes, NJ) and 20 g L<sup>-1</sup> urea (Fisher Scientific, Inc., Pittsburgh, PA) in

deionized water. The biocementation medium (calcium containing medium, CMM+) contained 3 g L<sup>-1</sup> Difco nutrient broth (BD, Franklin Lakes, NJ), 10 g L<sup>-1</sup> ammonium chloride (Fisher Scientific, Pittsburgh, PA), 20 g L<sup>-1</sup> urea (Fisher Scientific, Pittsburgh, PA), and 48 g L<sup>-1</sup> calcium chloride dihydrate (Fisher Scientific, Pittsburgh, PA) in deionized water. The growth medium (calcium free medium, CMM-) used for the urea batch study contained 3 g L<sup>-1</sup> Difco nutrient broth (BD, Franklin Lakes, NJ), 10 g L<sup>-1</sup> ammonium chloride (Fisher Scientific, Pittsburgh, PA), and 20 g L<sup>-1</sup> urea (Fisher Scientific, Pittsburgh, PA) in deionized water and was adjusted to pH 6.3. All solutions were filter-sterilized using SteriTop 0.2 μm bottle top filters.

# 2.1.3 Molds for generating biocemented structures

Interlocking molds for biocementation were designed with OnShape software and printed with a Prusa 3D Printer using Polylactic Acid (PLA) filament. Molds were designed with vertical slits of 0.4 mm width to facilitate transport of bacterial suspensions and cementation medium (**Figure S1**). The inside dimensions of the molds measured 50 x 50 x 50 mm<sup>3</sup>. Prism shape molds with dimensions of 90 x 25 x 25 mm<sup>3</sup> were also designed with vertical slits of 0.4 mm.

#### 2.2 APMDES treatment of sand

3-Aminopropyl-methyl-diethoxysilane (APMDES) (Gelest Inc., Morrisville, PA) was used to functionalize the sand surface. APMDES forms a monolayer of aminosilanes and thus confers positive charges to the treated surface <sup>25</sup>. This monolayer would be expected to maximize the number of active locations for electrostatic interactions with negatively charged cells. After the initial acid wash and autoclaving, sand was sonicated in acetone for 15 min and then in ethanol for another 15 min to remove carbon contaminants from the surface. The sand was dried at 100 °C on a hot plate, and then placed in a UV Ozone chamber (BioForce NanoSciences, Ames, Iowa) for 15 min to increase hydroxyl (-OH) moieties and active sites for APMDES attachment, and subsequently immersed in a solution of 1 % v/v APMDES in ethanol for 24 h. Sand was removed from the APMDES solution, rinsed in ethanol for 25

min to remove excess APMDES, and baked in an oven at 120 °C to remove polymerized APMDES on the surface.

X-ray photoelectron spectroscopy (XPS, Physical Electronics 5600) was used to verify the surface chemistry of APMDES-treated sand. XPS was conducted under ultra-high vacuum conditions ( $\sim 8 \times 10^{-10}$  Torr) using a monochromatic Al K $\alpha$  X-ray source (1486.6 eV photons) by monitoring the N 1s line and the chemical shifts associated with  $-NH_2$  and  $-NH_3^+$  species. Zeta potential measurements (Zeta-Meter System 4.0, Staunton, VA 24402) were used to confirm the surface charge of the sand after functionalization. Zeta potential was measured in neutral pH, deionized water, and data was collected for 50 sand grains per condition (untreated, APMDES-treated). XPS analyses were conducted to evaluate the quality and consistency of APMDES treatment of the initial batches as a proof of concept. The zeta potential was used again to confirm the functionalization of subsequent batches.

# 2.3 Determining the effect of APMDES treatment on microbial growth, viability, and urea hydrolysis

A 1 ml cryovial of thawed frozen *S. pasteurii* base stock (ATCC 11859) was added to 100 ml of BHI with 2% urea in an autoclaved 250 ml Erlenmeyer flask and incubated for 24 hours on the orbital shaker at 150 rpm at 30 °C. 1 ml of starter culture was transferred into 100 ml of fresh BHI with 2% urea medium and incubated overnight (16 hours). After the growth, approximately 40 ml of overnight culture was added to two 50 ml centrifuge tubes centrifuged at 6000 rpm for 10 minutes at 4°C. The supernatant of both tubes was decanted and resuspended in CMM-. The optical density was adjusted to 0.4 by diluting in sterile CMM-. 200µl aliquots were transferred to a 96-well plate, and OD<sub>600</sub> was measured using a Synergy HT reader (Biotek Instruments, Inc., Winooski, VT). The average OD<sub>600</sub> of sterile media (CMM-) was subtracted from the OD<sub>600</sub> of bacterial culture to measure the OD<sub>600</sub> of the culture without influence from the media or the 96 well plates.

To evaluate the effects of APMDES treatment on urea hydrolysis, microbial growth and pH, 10 grams of sand, APMDES-treated (n=3) and untreated (n=3) were mixed with 100 ml CMM- and

inoculated with 2 ml of the prepared bacterial cell suspension before being incubated at 30 °C on the orbital shaker at 150 rpm. Abiotic controls were prepared with 10 grams of APMDES-treated sand (n=1) and untreated sand (n=1) in CMM-. To make APMDES exposed media, 10 grams of APMDES-treated sand was pre-mixed with 100 ml of CMM- media in 250 ml Erlenmeyer flask and incubated overnight on the orbital shaker at 30 °C at 150 rpm, then filter-sterilized using SteriTop 0.2 μm bottle top filters and inoculated with 2 ml bacterial suspension to evaluate the toxicity of treatment on microbial growth.

Aliquots (1.5 ml) were collected in microcentrifuge tubes at each time point of 0, 1, 2, 4, 8, 12, 24, and 48 hours to measure urea concentrations, optical density, and pH. Sixty (60) microliter-aliquots from microcentrifuge tubes were diluted in 540 μL of 1.2M sulfuric acid (Fisher Scientific, Inc., Pittsburgh, PA) for a final dilution of 1:10 to use in a modified Jung Assay to determine the urea concentration <sup>26</sup>.

Microbial viability after exposure to APMDES was evaluated by plating cultures. An overnight *S. pasteurii* culture was centrifuged at settings 2210 rpm for 10 min at 4°C. The supernatant was removed and resuspended in phosphate buffered saline solution (PBS) to provide bacteria with a stable environment and prevent interference by potential growth in fresh growth media. The optical density was adjusted to 0.06 by adding fresh PBS to the residual pellet. A control that contained no sand was also prepared. One ml of the *S. pasteurii* inoculum (OD 0.06) was added to 9 ml of PBS and diluted up to 10<sup>g</sup>-fold. Five 10 μl samples from each dilution were plated on BHI agar plates and incubated at 30°C for 24 hours before colony-forming units (cfu) were counted for dilutions resulting in 3 to 30 colonies <sup>27</sup>. 1.85 grams of sand, APMDES-treated (n=3) and untreated (n=3), were added to 15 ml centrifuge tubes and inoculated with 3 ml of *S. pasteurii* culture in PBS (OD=0.06). The treatments were incubated for 1 hour on the benchtop before 1 ml of the supernatant was sampled from all treatments and serial dilutions and plating were performed. Following this step, for all centrifuge tubes containing sand, the microbial suspension was removed, sand was rinsed with 1 ml PBS to remove loosely attached microbes, and 3 mL of PBS were added back into the tubes. All centrifuge tubes underwent a vortex-sonicate-vortex step (30 seconds for each) to detach microbes from sand. Serial dilutions and plating were once again conducted

after detachment for groups containing *S. pasteurii*. Plates were incubated upside down in a 30°C incubator for 24 hours and colony-forming units were recorded.

The influence of APMDES treatment on bacterial cell membrane integrity was evaluated through live/dead staining and confocal laser scanning microscopy imaging. After immersion in bacterial suspension (OD<sub>600</sub>=0.6), sand samples were removed at 0h and 1h to investigate the effects of the APMDES treatment on cell membrane integrity. Samples were stained with 200 μL of a diluted 1:1 mixture of SYTO® (live/green) and Propidium Iodide (red/membrane compromised) (LIVE/DEAD BacLight Bacterial Viability Kit stain) (Invitrogen, catalog #L7012). Samples were rinsed three times with 200 μl Milli-Q water to remove excess dye and stored in the dark until imaging. Images were acquired with an upright Leica SP5 Confocal Laser Scanning Microscope (CLSM) using a 25X water immersion objective. The Argon laser at 488 nm was used to excite off the fluorescent signal from viable cells (green color), and the signal was detected using photomultiplier tube detection (PMT) between wavelengths of 495 and 550 nm. The fluorescent signal from membrane-compromised cells (red color) was captured by excitation at 561 nm and PMT detection between 595–650 nm. A laser beam scanned an area of interest at a frequency of 600 Hz.

## 2.4 Determining the effect of APMDES treatment on microbial attachment to sand grains

Scanning electron microscopy (SEM, Zeiss Supra 55VP) was used to investigate the surface microstructure and morphology of sand grains after immersion in bacterial suspensions and exposure to biocementation media. Elemental composition was obtained using an AZtec EDX (Oxford Instruments) detector. To investigate the microbial attachment on sand grains, 0.6 g of sand was inoculated with each 1 ml bacterial suspension (OD<sub>600</sub>=0.6) in microcentrifuge tubes, then the bacterial suspension was removed at 0.25h, 1h, and 16 h using a pipette, and samples were left to air dry at room temperature. Air-dried samples were mounted on SEM stubs using conductive carbon tabs (PELCO®, Ted Pella, Inc, Ca) and sputter coated with gold (Ted Pella 108 Carbon Coater) for 45 seconds to increase conductivity for high-resolution imaging.

## 2.5 Preparation of biocemented cubes

A starter culture was prepared by thawing 1 mL of frozen *S. pasteurii* base stock (ATCC 11859) and adding it to 100 mL of autoclaved BHI in a 250 mL Erlenmeyer flask. The flask was incubated for 24 h on an orbital shaker at 150 rpm at 30 °C. A fresh bacterial culture was then made by diluting the starter culture to 1:100 in sterile BHI and incubating for an additional 24 h on the orbital shaker table at 150 rpm. The culture volume was approximately 50% of the flask volume to provide oxygen for optimized bacterial growth. After 24 h, the optical density at 600 nm (OD<sub>600</sub>) was measured from 200µl aliquots in flat-bottom 96 well plates using a Synergy HT reader (Biotek Instruments, Inc., Winooski, VT). The average OD<sub>600</sub> of sterile BHI was subtracted from the OD<sub>600</sub> of bacterial culture, and the OD<sub>600</sub> of the culture was adjusted to 0.6 by diluting in sterile BHI.

Biocemented cubes were manufactured using APMDES-treated sand and untreated sand. First, 3D-printed cube molds were filled with 185 g of sand. Replicates (n=5) were prepared for each condition. Each mold was immersed in 300 mL of bacterial suspension (OD<sub>600</sub>=0.6) for 16 h and then in biocementation medium for 8 h. Biocementation was carried out by repeating the above immersion procedure (16h in bacterial suspension and 8h in biocementation media) for 3 and 7 days at room temperature using freshly made bacterial suspensions and biocementation media. To measure urea concentration using the Jung Assay protocol, 60 μL-aliquots were collected from biocementation medium at 0, 1, 2, 4, and 8h and diluted into 540 μL of 1.2 M sulfuric acid (Fisher) for a final dilution of 1:10 <sup>26</sup>. Specimens were de-molded, rinsed under tap water, and left to dry at 60 °C for a week. The weight of the cubes was recorded over time, until the equilibrium was reached. Additional specimens were manufactured as 25x25x90 mm<sup>3</sup> prisms (Figure 9C).

### 2.6 Determination of compressive strength

Biocemented cubes were subjected to unconfined compression testing in accordance with ASTM D2166/D2166M. The specimens were subjected to compression until failure using a constant load rate of

0.013 kN/s on an MTS Criterion Model 64. All replicates (n=5) for each condition were tested, and the height and area of each cube were recorded prior to testing.

### 2.7 Evaluation of biomineral content and mineralogical characteristics

After compressive strength testing, biocemented cubes were acid digested to estimate calcium carbonate content. Samples were collected from the edge (n=4) and middle (n=3) regions per cube. Two (2) grams of sample were placed in a 15 mL centrifuge tube, and 10 mL of 10% nitric acid were added to each tube and incubated at room temperature for 24 h to digest calcium carbonate. Calcium concentrations were measured in the supernatant, the remaining supernatant was removed, and the samples were allowed to dry at 60 °C for 72 hours prior to assessing the final mass. The obtained dry mass was used to calculate the weight percent of precipitated CaCO<sub>3</sub>.

Subsamples of the biocemented cubes were ground to fine powder using a pestle and mortar for XRD analyses. Crystalline phases of precipitated calcium carbonate on sand particles were examined using a Bruker D8 Advance Powder X-ray Diffractometer with Cu-K $\alpha$  source ( $\lambda$  = 1.54060 Å) at 40kV and 40mA; samples were scanned at angles from 5° to 75°, with a step size of 0.2°. The NIST Inorganic Crystal Structure Database (ICSD) was used to identify crystal structure data.

Small pieces of cubes biocemented for 7 days were embedded in epoxy (Ted Pella INC.) to compare the size distribution of biocemented bridges on untreated and APMDES-treated sand. Embedded biocemented chunks were sectioned using a low-speed diamond saw (Isomet, Buehler, Lake Bluff, IL) and polished with 600 and 1200 grit wet silicon carbide paper (Buehler, Lake Bluff, IL), then polished with Rayon fine cloths and different grades of alumina pastes (9, 5, 3, 1 µm). Sections were sonicated in tap water between polishing steps to remove impurities from the surface. Embedded sections were mounted on SEM stubs and carbon-coated (108C Auto SE Carbon Coater, Ted Pella INC.) to avoid charging artifacts for SEM-EDS analysis. Elemental maps were generated for calcium and silicon at three randomly selected locations, each for three replicates of 7-day treated and untreated cubes (Zeiss Supra55VP, working distance = 8.5, accelerating voltage = 10kV, magnification 200x).

SEM-EDX elemental maps were processed with custom MATLAB code to identify and measure sand grains (i.e., silicon-rich areas) and biomineral bridges (i.e., calcium-rich areas) (**Figure S2**). Images were binarized, thresholded using Otsu's method <sup>28</sup>, subjected to dilation and erosion steps, and filtered to remove objects with areas less than 20 pixels. Measures included biomineral bridge areal number density, the ratio of biomineral bridge area to sand grain area, and mean biomineral bridge area, major axis, minor axis lengths, and circularity (minor / major axis lengths).

## 2.8 Statistical Analysis

CaCO<sub>3</sub> content and compressive strength outcomes were compared between APMDES-treated sand and untreated sand using ANOVA. Three-factor mixed model ANOVA tested whether the weight percent of precipitated CaCO<sub>3</sub> depends on APMDES treatment, region, injections, and the interaction of these factors. Two-factor ANOVA tested whether compressive strength depends on APMDES treatment, the number of injections, or their interaction. To test the impact of calcium content on compressive strength, a linear mixed model was used with random effects of treatment and injections and a covariate of calcium content (analysis of covariance, ANCOVA). The influence of treatment on biomineral bridge characteristics was tested using mixed-model ANOVA with sample location as a random factor. All models were checked for residual normality and equal variance. If necessary, dependent variables were transformed to satisfy these assumptions. The statistical significance was defined *a priori* as p < 0.05. In the case of significant interactions in ANOVA models, post-hoc tests were performed using a Fisher's least significant difference (LSD) test with family-wise error controlled using the Bonferroni procedure (*i.e.*, critical alpha adjusted to 0.05 / number of comparisons (2) = 0.025). Minitab (ver. 19.2020.1) was used for statistical analyses.

# 3. Results and Discussion

3.1 APMDES treatment changes the surface properties of aggregates and localizes bacteria on these surfaces

Silane coupling agents, including APMDES and other closely related treatments, have been used to achieve bio-trapping on a variety of surfaces, such as silicon and glass wool fibers, for non-biocementation applications <sup>16,22–24,29</sup>. This method of 'bio-trapping' bacteria does not cause strict immobilization unless coupled with antibodies but instead localizes (bio-traps) bacteria within regions of treated surfaces, allowing bacteria to move freely near the surface of the sand particles <sup>16</sup>.

XPS analysis was performed to confirm the elemental composition of aggregates before and after APMDES treatment. The XPS survey spectra of untreated sand showed the presence of Si (2p and 2s), O (1s), and C (1s) signals; the spectra of the APMDES-treated sand additionally revealed peaks at 399.6 eV corresponding to N (1s) amine groups, confirming the presence of amine moieties on the APMDES-treated sand (Figure 1 A).

The amine groups (in particular, quaternary amine moieties) imparted a positive charge on sand surfaces. A change in zeta potential also indicated successful functionalization. The zeta potential of untreated sand was -28.18 mV, and APMDES-treated sand was +36.47 mV (**Figure 1 B**). Since the zeta potential of *S. pasteurii* is -67 mV <sup>30</sup>, electrostatic interactions between the positively charged APMDES-treated sand surface and the negatively charged wall of *S. pasteurii* likely promote bacterial trapping.

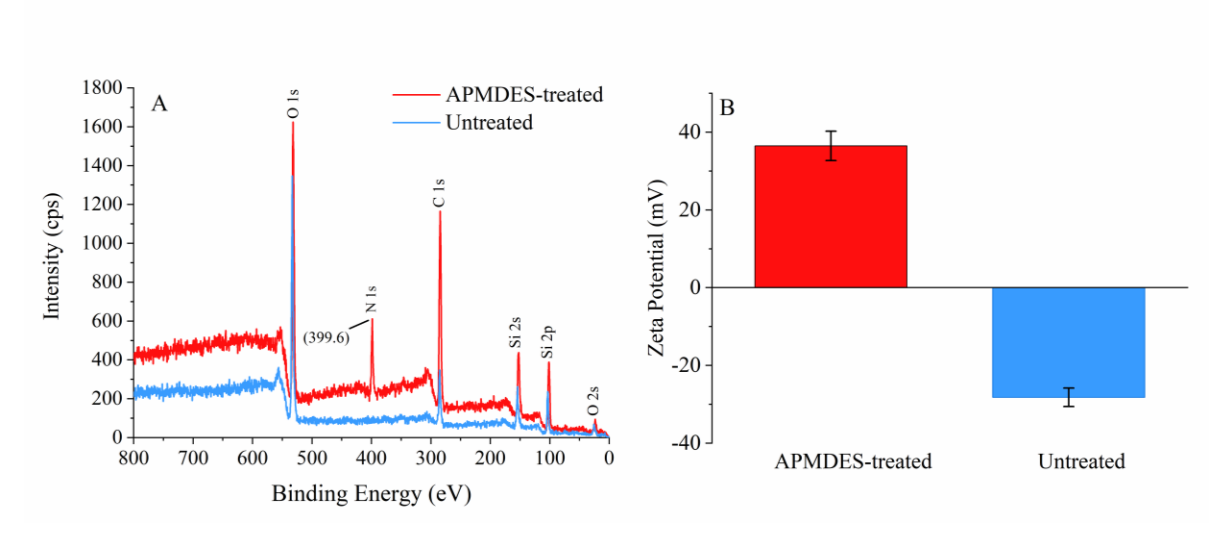


**Figure 1**. Change in surface properties of sand with APMDES treatment. **A)** X-Ray Photo Electron Spectroscopy (XPS) of sand grains before and after APMDES treatment confirming the presence of amine groups with the peak at a binding energy of 399.6 eV (N1s). **B)** Zeta potential measurements of sand grains in distilled water, a neutral pH of 7, before and after APMDES treatment, n=50 sand grain per group. Error bars represent 1 standard deviation.

Imaging data confirmed the immediate localization of *S. pasteurii* on APMDES-treated sand surfaces, which under scanning electron microscopy (SEM) appeared as a thin layer of cells (**Figure 2**). The bacterial attachment at 0.25h, 1h, and 16h after immersion in bacterial suspension was greater on the APMDES-treated sand than on the untreated sand. This length of time study was chosen because it represents the length of a biocementation treatment in this study (16 hours). SEM micrographs showed few cells attached to untreated sand at 0.25h, 1h, and 16h of immersion (**Figure 2A-C**). By contrast, APMDES-treated sand showed nearly instantaneous bacterial adhesion at 15 minutes, abundant bacterial adhesion after 1h of immersion, and a dense layer of microbes at 16h (**Figure 2D-F**).

Together, these data confirm that APMDES treatment was successful in bio-trapping bacteria on sand surfaces for time periods relevant to bacterial biocementation. This work is the first demonstration of the effective use of APMDES on sand surfaces. Sand is a common substrate for MICP-based biocementation that has many applications, such as manufacturing building materials and strengthen soils

<sup>7</sup>. Employing APMDES in the biocementation process would be expected to be useful for many of these applications where efficiency of biomineralization and/or strength development is appreciated. Whether APMDES would work as successfully on other types of aggregates was not investigated here but would be a valuable investigation.

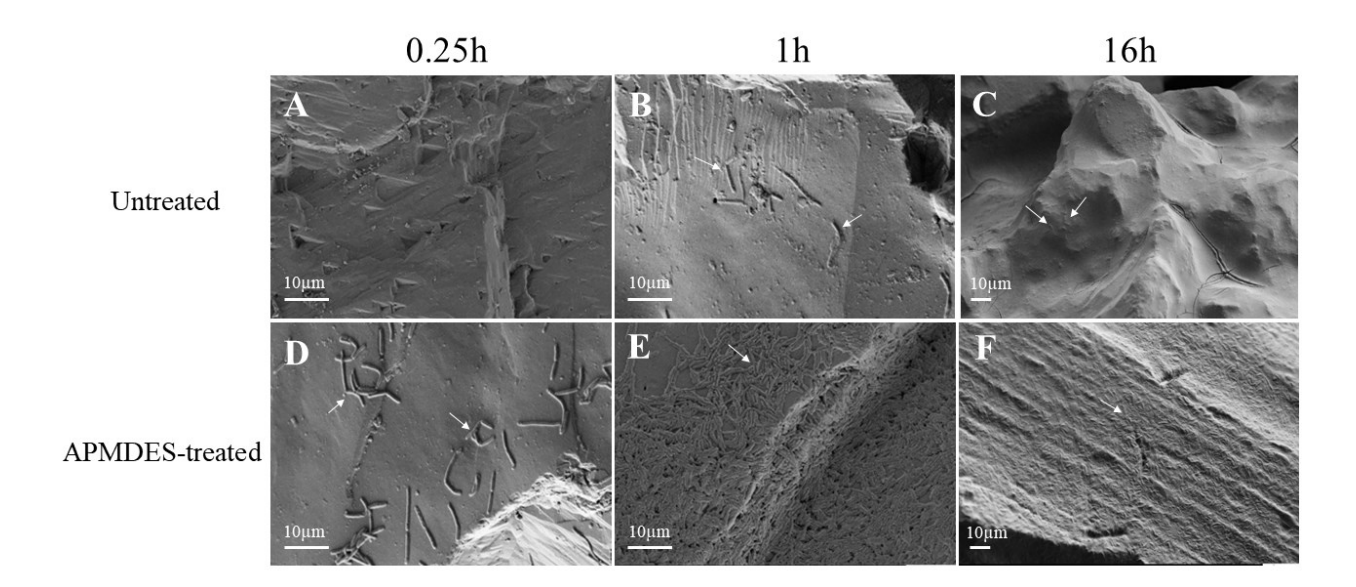


**Figure 2.** Initial attachment of *S. pasteurii* on APMDES-treated and untreated sand. A-C) SEM indicates sparse attachment of microbes on untreated sand at 0.25h and 1h and almost no attachment after 16h of immersion. D-F) APMDES-treated sand shows abundant attachment of microbes to the sand surface at 0.25h, 1h and 16h of immersion. At 1hr and 16h, the microbes are seen as a dense mat. Scale bars are 10 μm. White arrows indicate *S. pasteurii*.

# 3.2 APMDES treatment inhibits bacterial viability and growth but does not impede urea hydrolysis during biocementation

A batch study was conducted to determine the influence of APMDES treatment on *S. pasteurii* growth and hydrolysis of urea. The optical density of the initial *S. pasteurii* inoculum was measured as 0.027. The growth curve of *S. pasteurii* in the presence of untreated sand was similar to the planktonic condition without sand, reaching an optical density of 0.2 at 8 hours. Bacterial growth was inhibited by the presence of APMDES-treated sand (**Figure 3A**), most likely due to the presence of  $-NH_3^+$  moieties,

which are expected to be toxic <sup>17,31</sup>. Growth was slightly inhibited by APMDES in solution. However, even in the presence of APMDES-treated sand, urea hydrolysis and the resulting increase in pH in solution still occurred, albeit at slower rates (Figures 3B-C). Twenty (20) g/L urea were almost completely hydrolyzed in 8 hours for conditions without APMDES, while APMDES-treated sand required 48 hours to hydrolyze most of the urea. The urea hydrolysis was likely slower in the presence of APMDES-treated sand because there was no bacterial growth that could increase the availability of the urease enzyme. This suggests that despite inhibiting bacterial growth, APMDES does not interfere substantially with the activity of the *S. pasteurii* urease.

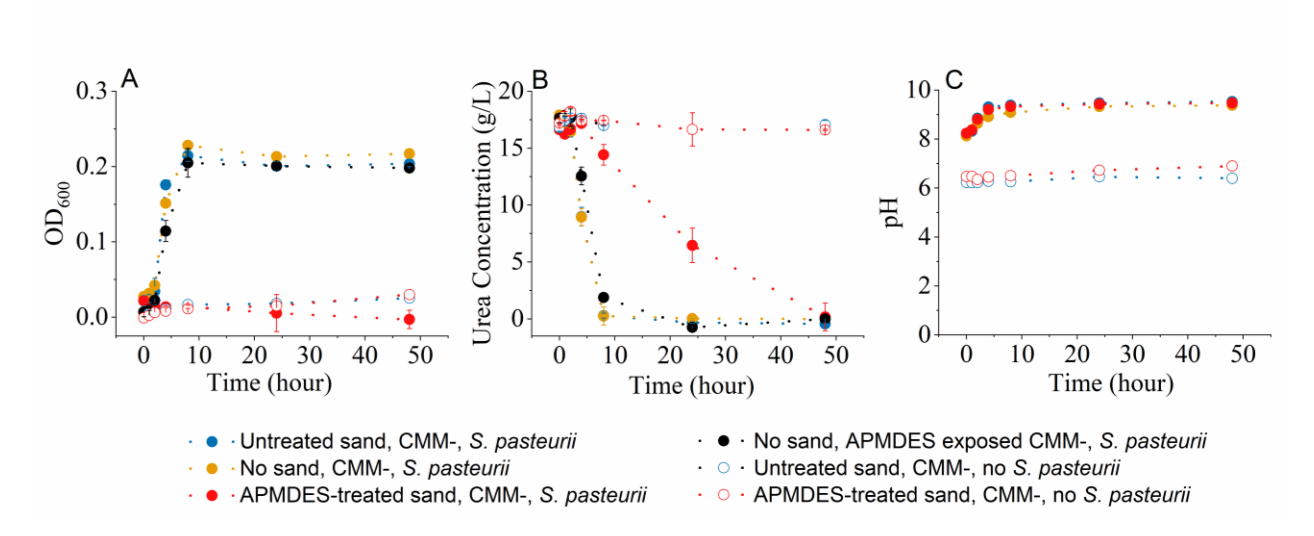


**Figure 3.** *S. pasteurii* growth, urea hydrolysis and pH in batch reactors over 48 hours. A) Optical density (OD) increased over time for positive controls but not for APMDES-treated sand, indicating inhibition of growth, B) Urea concentration decreases rapidly for positive controls and also decreases, although less rapidly, for APMDES-treated sand, and C) pH increased for all microbial cultures, regardless of APMDES treatment, which is expected during urea hydrolysis.

After establishing that APMDES impeded *S. pasteurii* growth, the impact of the treatment on viability was assessed. Viability was determined from flask solutions before and after attempting to detach *S. pasteurii* from sand using a vortex-sonicate-vortex procedure. In the untreated condition, an abundance of viable *S. pasteurii* cells were detected before and after the vortex-sonicate-vortex procedure

for both planktonic cultures and for microbes attached to untreated sand (**Figure 4**). Solutions were replaced between the initial measurement and detached conditions, ensuring that viable microbes measured after the vortex-sonicate-vortex steps had detached from sand. By contrast, no culturable cells were detected in APMDES-treated sand before or after the vortex-sonicate-vortex procedure. SEM images indicated that there was an abundance of microbes attached to sand in the APMDES-treated condition, both before and after the vortex-sonicate-vortex procedure (**Figure 5**). These results indicate that APMDES treatment results in strong attachment of *S. pasteurii* cells that resist detachment from sand, and that *S. pasteurii* was not culturable under these conditions.

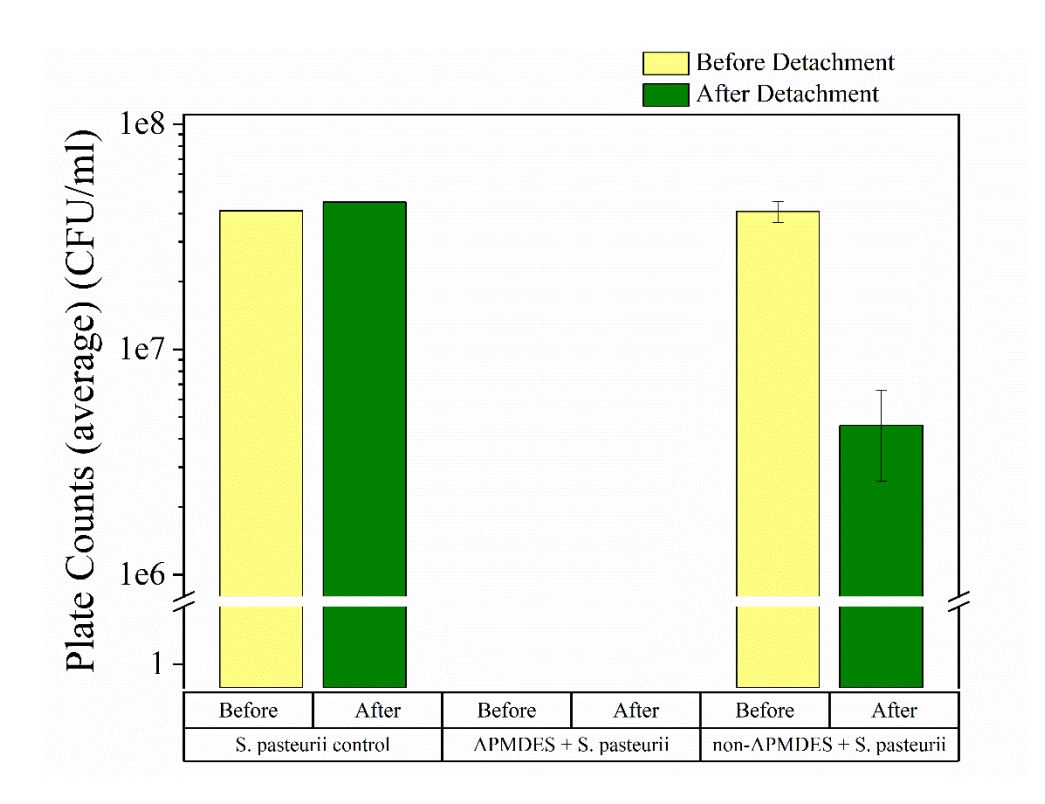


**Figure 4.** Plate counts of *S. pasteurii* from supernatant before and after vortex-sonicate-vortex induced detachment from sand, indicating that APMDES treatment of sand causes a loss of *S. pasteurii* viability.

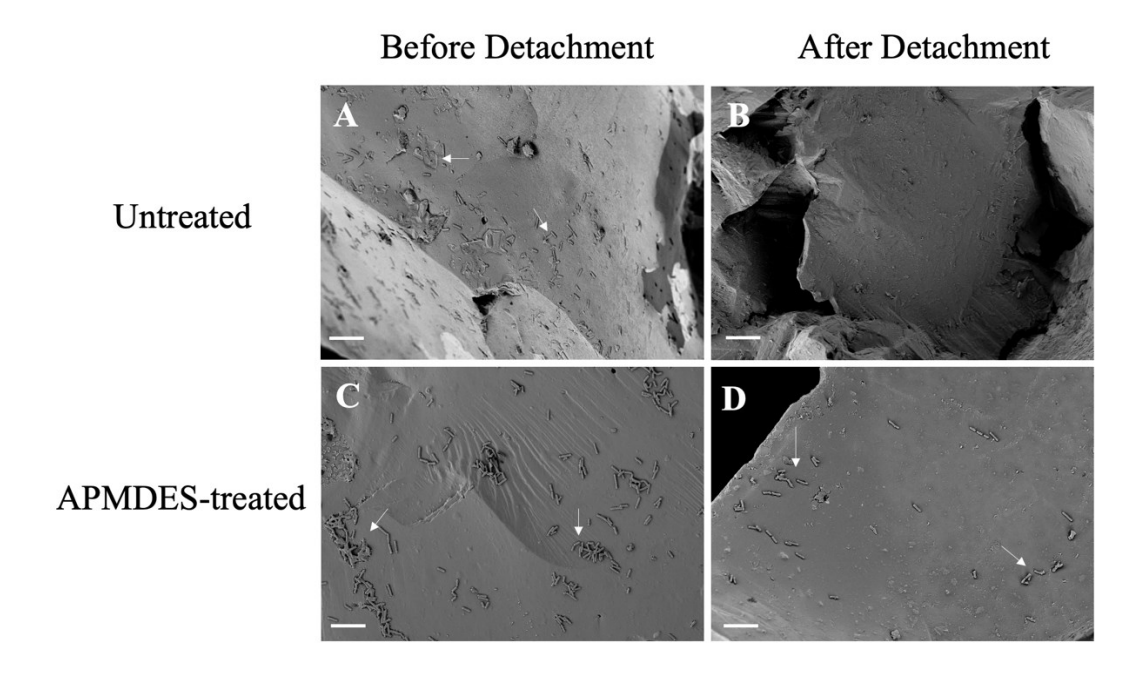


**Figure 5.** *S. pasteurii* cells were imaged on the surface of APMDES-treated and untreated sand, before and after detachment of microbes. A-B) Untreated sand appears to have less microbes attached to its surface before and after detachment. C-D) SEM images indicate higher numbers of microbes attached to APMDES-treated sand, both before and after the vortex-sonicate-vortex-induced attempt to detach microbes from sand surfaces. Scale bars are 10 μm. White arrows indicate *S. pasteurii* 

An additional imaging study was performed to visualize the impact of APMDES treatment on *S. pasteurii* at early time points. Confocal laser scanning microscopy (CLSM) was performed soon after *S. pasteurii* exposure to APMDES-treated sand (15 minutes) and 1 hour after exposure (**Figure 6**). CLSM images showed green (Syto9 stained, non-membrane-compromised cells) and red (propidium iodidestained, membrane-compromised cells). Untreated sand showed very few cells at 15 minutes and sparse but mostly non-compromised (green) cells at 1 hour (**Figure 6A-B**). By contrast, APMDES-treated sand had abundant cells attached at both time points, with a small fraction of viable (green) but mostly membrane-compromised cells (red) (**Figure 6C-D**). Importantly, impaired membrane integrity visualized through this method can, but does not always, indicate impaired cell viability <sup>32,33</sup>.

Together, these data indicate that APMDES is detrimental to *S. pasteurii* viability and growth. There are several potential reasons that may explain this effect. The increased electrostatic attraction between the cells and the treated surfaces could cause cell membrane damage. In support of this possibility, in other settings, positively charged surfaces have been reported to have antimicrobial effects due to strong electrostatic interactions disrupting cell membrane integrity 16,18,31,34,35

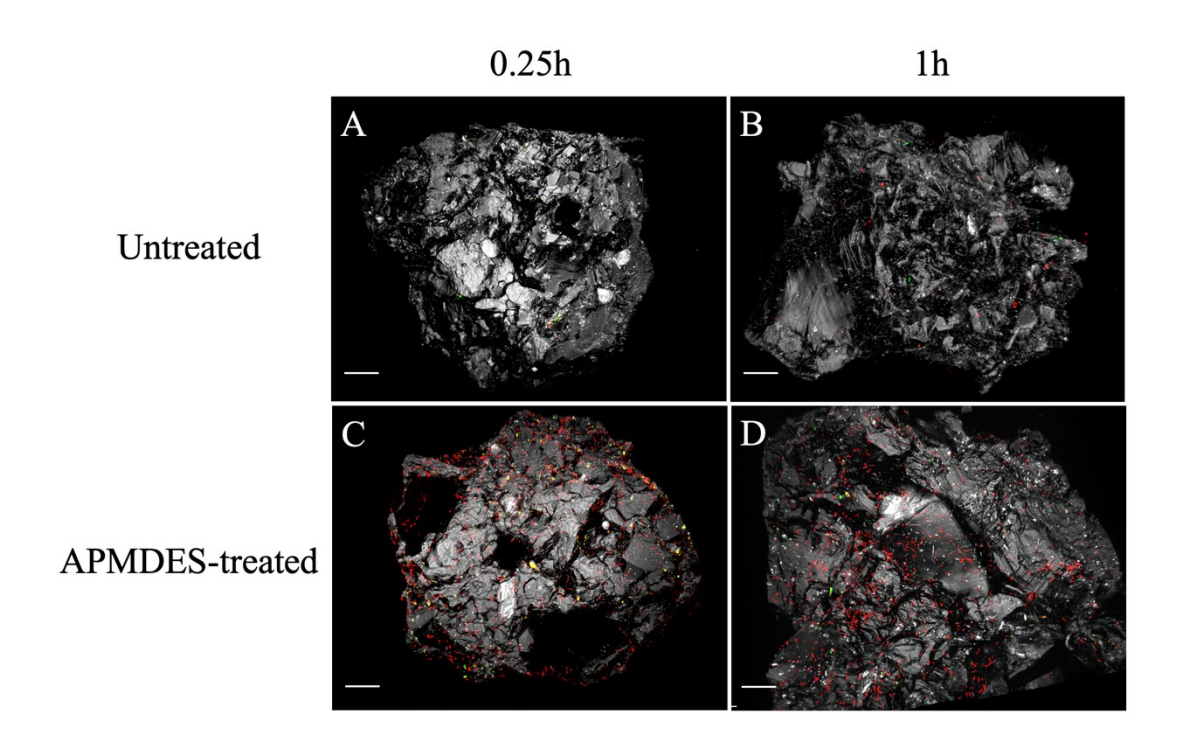


**Figure 6.** Initial attachment of *S. pasteurii* on APMDES-treated and untreated sand. A-B) CLSM images demonstrate sparse, but predominantly viable (green) microbes attached to untreated sand at 0.25h and 1h. C-D) Abundant microbial attachment is apparent on treated sand, with a mixture of viable (green) and membrane-compromised (red) microbes. Scale bars are 30 μm.

Though APMDES treatment was detrimental to the growth and viability of *S. pasteurii* (**Figures** 3, 4, and 6), calcium carbonate precipitation still occurred reliably on APMDES-treated sand. The decrease in urea concentrations over time in the bulk fluid during daily 8-hour long biocementation

periods indicated that urea hydrolysis was equivalent in both APMDES-treated sand and untreated sand conditions (**Figure 7**), suggesting that the survival of cells exposed to APMDES was not necessary for urea hydrolysis and biocementation. Importantly, cells and media were injected several times into both untreated and treated conditions, and the negative effects of APMDES on the viability of cells may decrease as the sand surface is increasingly covered with minerals.

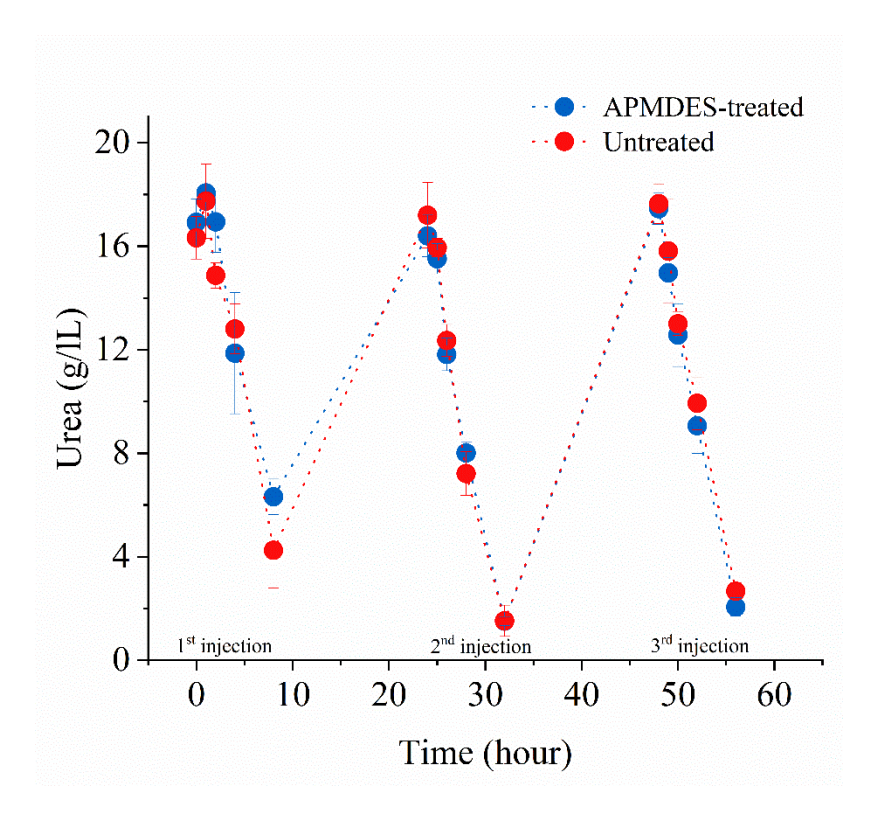


**Figure 7.** Urea concentrations (measured using a modified Jung assay) over time in the presence of APMDES-treated sand and untreated sand. Urea was added to an initial concentration of 20g/L urea each day and was almost completely hydrolyzed during the 8-hour time period.

The finding that urea hydrolysis does not depend on *S. pasteurii* viability in APMDES-treated conditions might contribute to the development of more efficient MICP processes, where the focus could be on urease enzyme functionality rather than maintaining high levels of cell viability. There are potential upsides for biocementation treatments that do not rely on preserving microbial viability. For example, the

use of microbes in situations (*e.g.*, outdoor usage) where their growth may disrupt the local soil microbiome may benefit from eliminating the viability of those cultures, whether through a treatment like APMDES or through another strategy (*e.g.*, heat treatment, isolating the urease enzyme, etc.).

## 3.3 APMDES treatment decreases the time required for strength development via biocementation

After determining that APMDES treatment increases attachment of ureolytic microbes to sand, the next question was whether APMDES would impact the efficiency of strength gain through biocementation. For both APMDES-treated and non-treated conditions, the minerals precipitated during biocementation were mostly calcite intermixed with minor fractions of vaterite, as confirmed by XRD (Figure 8). However, the appearance of cube and prism structures was markedly different with the APMDES treatment. Structures manufactured using APMDES-treated sand had much more precise edge definition than those made using untreated sand (Figure 9).

APMDES improved the compressive strength of cube specimens compared with the untreated condition (+49.7%, p = 0.007) (**Figure 10, Table S1**). After 3 injections, the mean compressive strength with APMDES treatment was almost double compared with untreated controls (2.31 vs. 1.23 MPa). There was not a significant effect of injections (p = 0.054) on compressive strength, nor a significant interaction between injections and treatment (p = 0.147). It is noted that it is likely that this study was underpowered to detect the expected increase in strength with more injections and that including additional specimens would be likely to increase statistical significance.

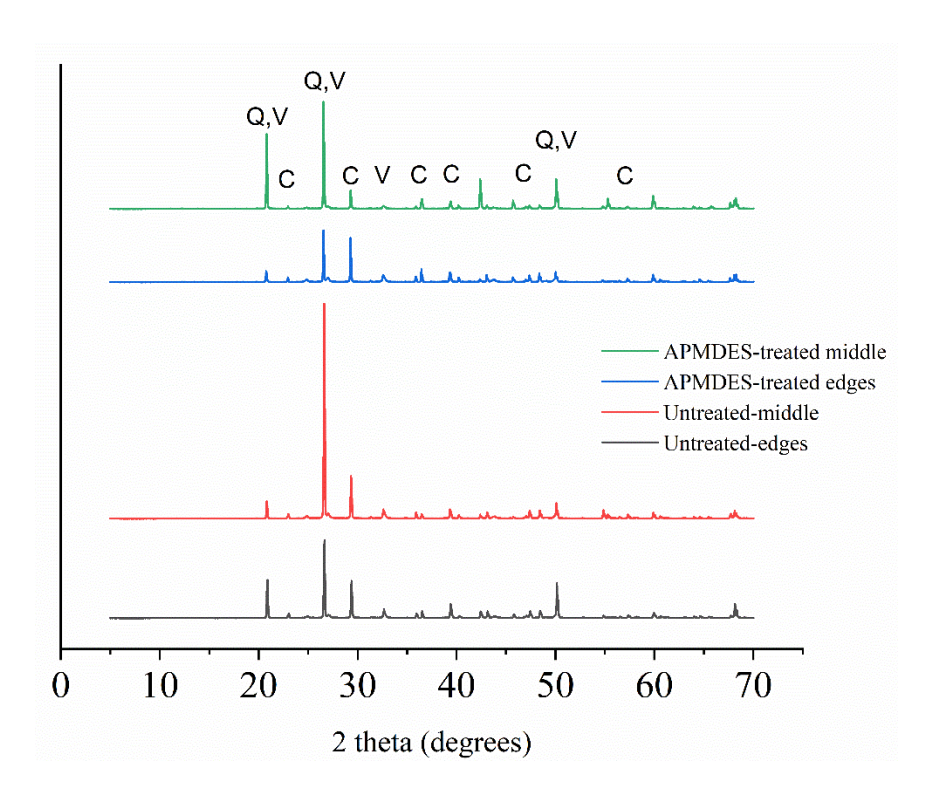


**Figure 8.** XRD spectra of 7-day biocemented cubes. Results reveal abundant calcite (C), with minor vaterite (V) presence. Note that the largest vaterite peak overlaps with quartz (Q), which is highly abundant for these samples.



**Figure 9.** Biocemented specimens after 3 injections. **A)** 50 x 50 mm cubes prepared using APMDES-treated sand. **B)** 50 x 50 mm cubes prepared from non-treated sand. **C)** Prisms (25 x 25 x 90 mm) prepared from APMDES-treated sand (left) and non-treated sand (right).

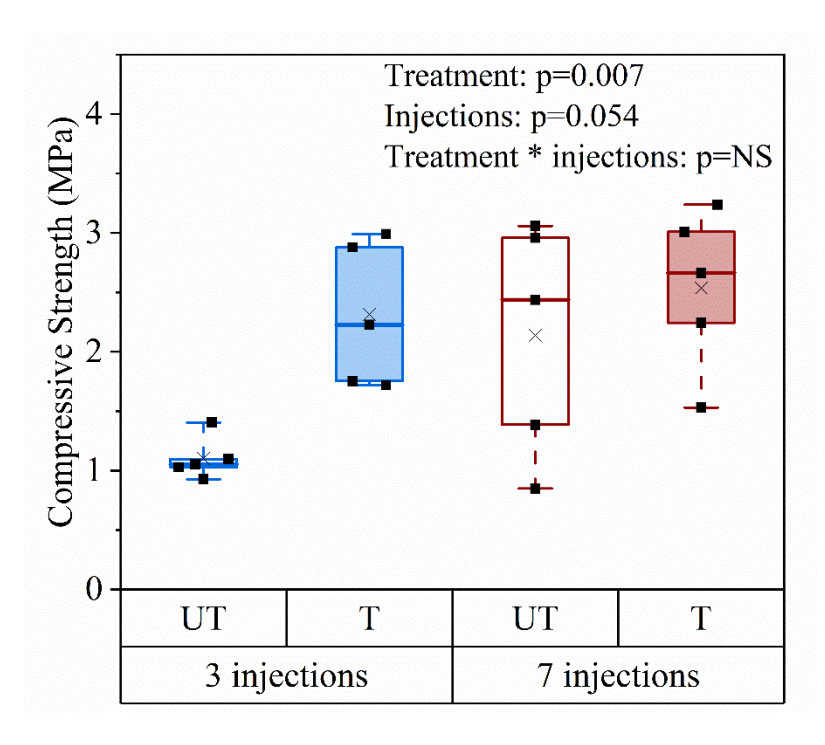


**Figure 10.** Compressive strength of APMDES-treated (T) and untreated (UT) cubes after 3 and 7 days of one injection daily. Boxplots show the median (line), mean (cross), interquartile range (box), minimum/maximum (whiskers), and individual data (dots).

The strength gain seen for APMDES-treated samples was rapid compared with the untreated controls as well as compared with data from other biocementation studies (**Figure 11**). For example, Bernardi and coworkers used *S. pasteurii* and urea-calcium medium to manufacture bio-bricks with dimensions of 91 mm x 58 mm x 200 mm. After 3 injections per day over 7 days (21 treatments), 14 days (42 treatments), or 28 days (84 treatments), they report achieving average compressive strengths of 0.07 MPa, 0.44 MPa, and 1.65 MPa, respectively <sup>36</sup>. Similarly, Lambert et al., 2019 developed brick-shaped specimens with dimensions of 222 mm x 106 mm x 73 mm using human urine as a urea source, which were biocemented for 8 days (6 injections per day, 48 treatments). This process produced specimens with an average compressive strength value of 2.7 MPa <sup>37</sup>. Bu et al. manufactured MICP-treated brick specimens with 177 mm x 76 mm x 38 mm dimensions, which had compressive strengths averaging 0.42 MPa after 1 treatment with 7 days of reaction <sup>38</sup>. There are important differences across these studies in the type of microorganism, solution chemistry, size of sand, and other characteristics that can influence compressive

strength. Regardless, APMDES treatment results in a very rapid strength development (average 2.1 MPa after 3 injections) compared to the most similarly shaped structures in literature. It is possible that additional injections beyond the endpoint of this study could further increase the strength of APMDES-treated materials, but this possibility requires additional investigation.

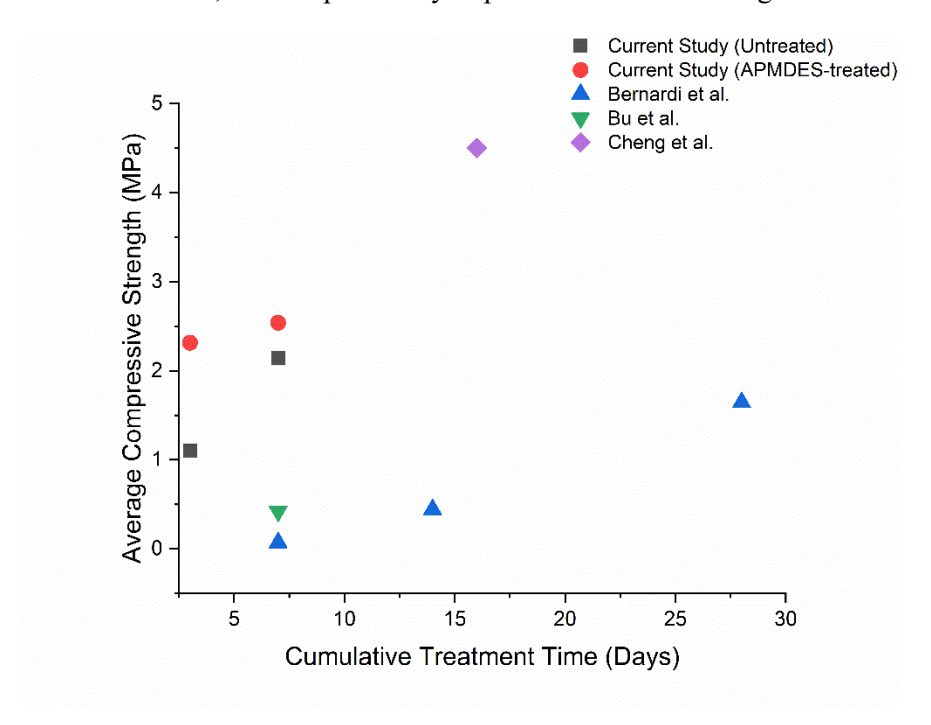


**Figure 11.** Relationships between cumulative MICP treatment time (days) and unconfined compressive strengths across findings from this study and other investigations. While all studies utilized silica sand, *S. pasteurii*, and similar constituents within biocementation media, there were differences in sand size, media concentration, and biocementation procedures, which are detailed in Table S4.

# 3.4 The strength gain from APMDES treatment is not solely explained by calcium-containing biomineral gain

Because compressive strength has been shown to have a positive correlation with CaCO<sub>3</sub> accumulation <sup>13,14,16</sup>, calcium-containing biomineral gain, which would be expected to largely represent CaCO<sub>3</sub> accrual, was estimated by acid digest (**Figure 12**). Biomineral gain depended on interactions between the number of injections and treatment (AMPDES vs. no treatment) or region (*i.e.*, edge or

middle) (**Figure 12A**). Region and injection had an interactive effect (p = 0.003) on the weight percent of calcium-containing biomineral gain. The outside (edges) of the cubes had more calcium-containing mineral compared to the center (middle) of the cubes manufactured with 3 injections (4.53% vs. 3.54%, p = 0.006) and 7 injections (7.63% vs. 4.06%, p < 0.001) (**Figure 12B, Table S2**). The effect of APMDES treatment was different between 3-day and 7-day injections (p = 0.015). APMDES-treated sand had a greater percentage of calcium-containing biomineral gain than untreated sand after 3 injections (4.46% vs 3.60%, p = 0.019), but calcium-containing biomineral gain was not different between APMDES-treated sand and untreated sand after 7 injections (p = 0.280) (**Figure 12C, Table S3**).

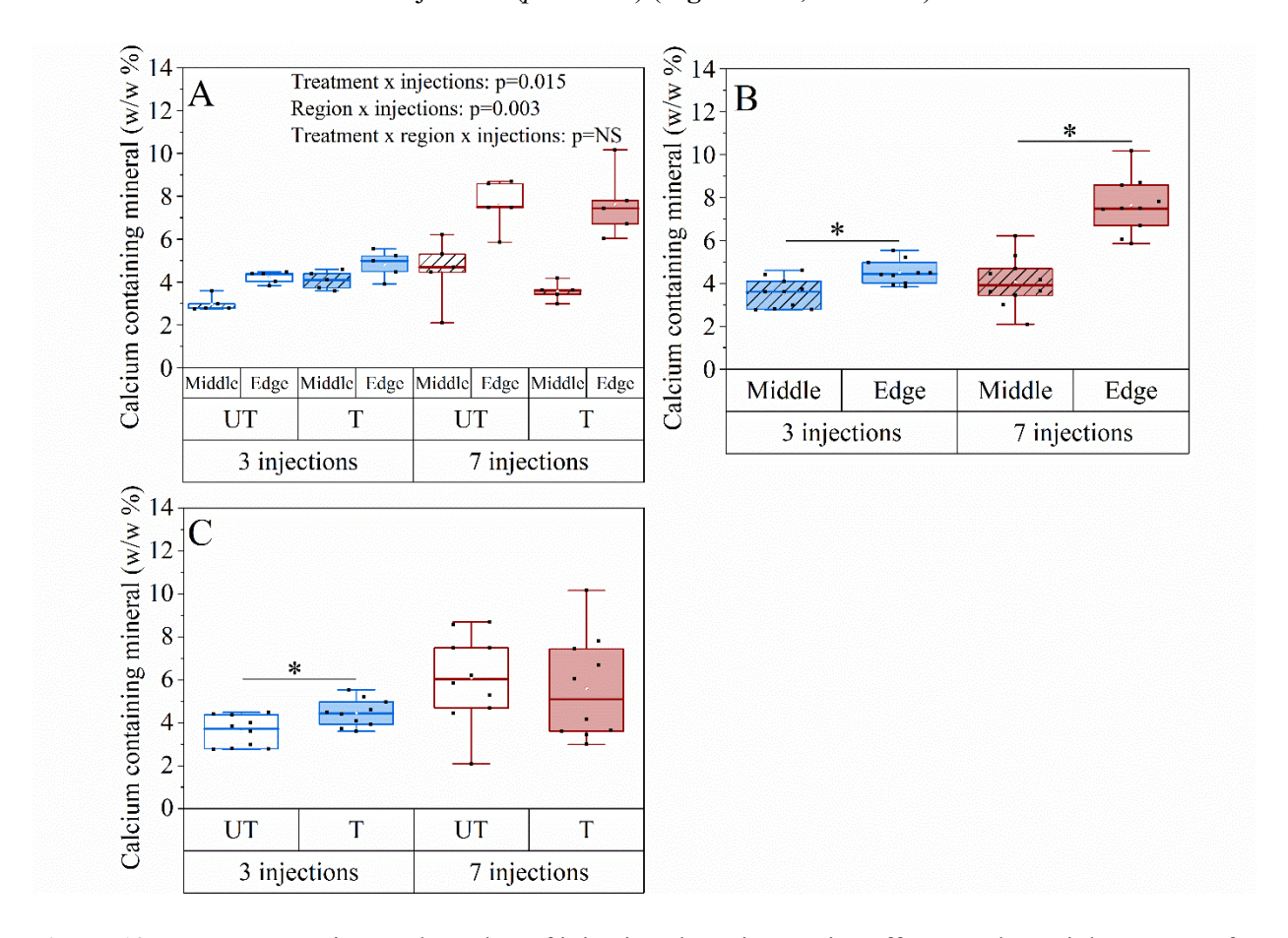


**Figure 12.** Treatment, region, and number of injections have interactive effects on the weight percent of calcium-containing mineral gain. A) Biomineral gain estimated from acid digests of edge and middle samples of sand cube specimens prepared with 3 or 7 injections. B) Region-injection interaction effect on % calcium-containing mineral. C) Treatment-injection effect on % calcium-containing mineral. Boxplots

show the median (line), interquartile range (box), maximum/minimum (whiskers), and symbols representing all data points (squares). Significant simple effects from post-hoc tests following significant interactions are indicated with asterisks.

Since APMDES increased strength at 3 injections and 7 injections but calcium-containing biomineral gain was only higher at 3 injections, analysis of covariance (ANCOVA) was used to test the relationship between strength and calcium gain. After accounting for the linear, positive relationship with calcium content through ANCOVA, there was still a significant effect of APMDES treatment on compressive strength (p = 0.029). These data demonstrate that strength gain with APMDES treatment is likely not solely attributed to greater accumulation of biomineral (**Figure 13**).

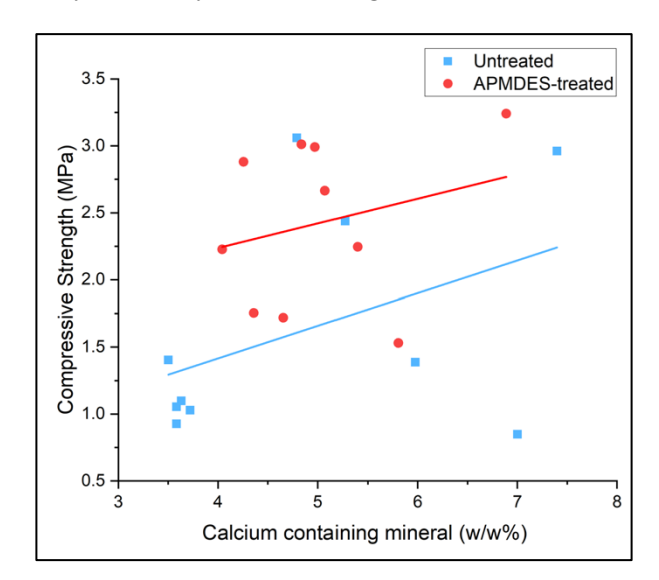


Figure 13. Mean calcium-containing biomineral gain versus compressive strength of specimens prepared with untreated ( $r^2 = 0.18$ ) or APMDES-treated ( $r^2 = 0.06$ ) sand combining 3 and 7 injection data. A regression line is shown for each condition.

Because APMDES treatment appears to alter the relationship between biomineral accumulation and strength gain, the geometry of biomineral bridges was investigated from embedded and polished sections of biocemented cubes. There were several statistically significant microstructural differences between the APMDES-treated and untreated conditions, such as increased sphericity and decreased size for calcium carbonate bridges in the APMDES-treated structure (**Table 1**). This result could indicate a

difference in how biomineral bridges nucleate and grow with APMDES treatment. Other measures were not significantly different between treated and untreated groups (**Table 1**).

**Table 1**. Biomineral bridge geometric characteristics from SEM-EDX maps of calcium (biomineral bridges) and silicon (sand grains) (**Figure S2**). Means were calculated from three specimens, which each represent the mean of three randomly selected regions of interest. Data are presented as mean  $\pm$  standard deviation.

Measure	Untreated	APMDES-treated	p-value
Mean total sand area	$22.99 \pm 1.39 \text{ mm}^2$	$24.60 \pm 0.88 \text{ mm}^2$	0.069
Mean number of sand grains	$39.33 \pm 2.52$	$38.56 \pm 3.47$	0.227
Mean total CaCO <sub>3</sub> area	$2.65 \pm 0.91 \text{ mm}^2$	$1.89 \pm 0.67 \text{ mm}^2$	0.189
Mean CaCO <sub>3</sub> area / sand area	$0.120 \pm 0.0490$	$0.0788 \pm 0.0302$	0.141
Mean number of biomineral bridges	$84.22 \pm 8.88$	$86.89 \pm 14.26$	0.295
Mean biomineral bridge number / sand grain number	$2.189 \pm 0.178$	$2.256 \pm 0.345$	0.837
Mean biomineral bridge area	$0.031 \pm 0.012 \text{ mm}^2$	$0.021 \pm 0.006 \ mm^2$	0.045
Mean biomineral bridge major axis	$0.29\pm0.048~mm$	$0.24 \pm 0.032 \ mm$	0.133
Mean biomineral bridge minor axis	$0.14 \pm 0.027 \ mm$	$0.11 \pm 0.015 \text{ mm}$	0.073
Mean biomineral bridge circularity (minor/major axes)	$0.49 \pm 0.050$	$0.55 \pm 0.029$	0.033

# 3.5. Implications for sustainability

Biocementation has garnered considerable attention as a lower-temperature process for building load-bearing materials or improving soils, but sustainability is decreased as the number of injections of bacteria and nutrients increases <sup>39</sup>. APMDES treatment may increase the sustainability of bacterial biocementation by decreasing the number of injections required to achieve a target compressive strength. Further, biocementation using ureolytic microbes produces ammonia, which is not desirable in some locations and situations. APMDES treatment has the potential to improve the sustainability of biocementation treatment by decreasing the number of inputs (*i.e.*, injections) and waste outputs. It is important to note that functionalizing the sand surface with silane coupling agents increases the energy requirements of creating

the biocemented structure, as the sand undergoes drying and ozone treatment steps, which require energy inputs. This treatment process also requires the production and disposal of chemicals, including ethanol, acetone, and APMDES. A full comparative life cycle analysis of APMDES treatment versus conventional biocementation was outside of the scope of the present investigation but would be valuable for comparing the two manufacturing methods.

#### 3.6. Limitations

This study has several important limitations. While the APMDES treatment was reported to increase strength development for similar biomineral content, the specific mechanisms contributing to this strength development require further investigation. Additionally, while microscopy images provided qualitative evidence of increased microbial density on APMDES-treated sand surfaces, it is not known whether the APMDES treatment and subsequent bacterial distribution were homogenous within all areas of the sand matrix. In this study, we did not investigate whether strength gain would continue past 7 injections, but this would merit future investigation. Furthermore, the dynamics of how microbial attachment, nucleation, and growth are impacted for the first treatment versus subsequent treatments are not answered here. Additional research is needed to gain a better understanding of how these treatments affect biomineral nucleation and growth and resulting strength development. Furthermore, prior experimentation with  $-NH_3^+$  moieties show that these ions are toxic to some bacteria but not to others  $^{34}$ . Additional careful study is required to identify combinations of bacteria and surface charges that achieve goals of either viability or non-viability, depending on the intended applications. Another limitation is that only silica sand was investigated in this study. The effectiveness of APMDES treatment to improve the efficiency of biocementation may vary with soil type and should be investigated in future work. More broadly, further work is required to explore the feasibility of utilizing APMDES treatment for larger-scale applications, including the potential simplification of treatment steps and also the study of cellular attachment and viability in these conditions.

#### 4. Conclusions

This study demonstrates that the use of amino silane coupling agents, such as 3-aminopropyl-methyl-diethoxysilane (APMDES), can be an effective method for improving the efficiency in strength development during bacterial biocementation. The key findings of this research were that APMDES treatment altered surface properties of sand, which resulted in increased attraction for ureolytic bacteria, and improved strength development over a shorter period of time. APMDES achieved this strength gain without increasing the quantity of calcium-containing biomineral within the structure, indicating an alteration of other characteristics contributing to strength. Overall, these results suggest that aggregate pre-treatment methods such as amino silane coupling agents may offer promising solutions for improving efficiency and effectiveness outcomes related to microbial biomineralization.

## **Supporting Information**

3D print model of molds, SEM-EDX map of biomineral bridges, effects of APMDES treatment on compressive strength, effects of number of injections and region on biomineral accumulation, effects of number of injections and treatment on biomineral accumulation. Comparison of experimental designs in highlighted studies

#### **Author Contributions**

G.E.U: Conceptualization, Methodology, Formal Analysis, Investigation, Data Curation, Writing-Original Draft, Visualization, Writing-Review-Editing

K.R: Formal Analysis, Investigation, Visualization Writing-Review-Editing

J.C.B: Software, Formal Analysis, Writing-Review-Editing

R.S.: Investigation, Visualization Writing-Review-Editing

R.A: Resources, Writing-Review-Editing

R.G.: Writing-Review-Editing, Supervision, Funding Acquisition

A.P.: Conceptualization, Resources, Writing-Review-Editing, Supervision, Funding Acquisition

C.M.H: Conceptualization, Formal Analysis, Resources, Data Curation, Writing-Original Draft, Writing-Review-Editing, Supervision, Project Administration, Funding Acquisition

## **Funding Sources**

The authors gratefully acknowledge support from the National Science Foundation (C.H., A.P., R.G.: 2036867; C.H., R.G., R.A: 2328351). Any opinions, findings, and conclusions, or recommendations expressed in this material are those of the authors and do not necessarily reflect the views of the National Science Foundation.

# Acknowledgements

The authors appreciate assistance from the staff of the Montana State University Center for Biofilm Engineering (Dr. Heidi Smith) and the Image and Chemical Analysis Laboratory (Dr. Sara Zacher). Imaging was made possible by the Center for Biofilm Imaging Facility at Montana State University, which is supported by funding from the National Science Foundation MRI Program (2018562), the M. J. Murdock Charitable Trust (202016116) and the US Department of Defense (77369LSRIP)." Additionally, the authors appreciate Kenna Brown's assistance in designing 3D-printed molds and Allyson Bomber's assistance with acid digesting.

## **Abbreviations**

APMDES, 3-aminopropyl-methyl-diethoxysilane; MICP, microbially induced calcium carbonate precipitation; BHI, brain heart infusion; CMM+, calcium containing medium; CMM-, calcium free medium; CLSM, confocal laser scanning microscope; PMT, photomultiplier tube; SEM, scanning electron microscopy.

#### References

- 1. Izumi Y, Iizuka A, Ho HJ. Calculation of greenhouse gas emissions for a carbon recycling system using mineral carbon capture and utilization technology in the cement industry. *J Clean Prod.* 2021;312:127618. doi:10.1016/j.jclepro.2021.127618
- 2. Teh SH, Wiedmann T, Castel A, de Burgh J. Hybrid life cycle assessment of greenhouse gas emissions from cement, concrete and geopolymer concrete in Australia. *J Clean Prod.* 2017;152:312-320. doi:10.1016/j.jclepro.2017.03.122
- 3. Achal V, Mukherjee A. A review of microbial precipitation for sustainable construction. *Constr Build Mater*. 2015;93:1224-1235. doi:10.1016/j.conbuildmat.2015.04.051
- 4. Zhang W, Zheng Q, Ashour A, Han B. Self-healing cement concrete composites for resilient infrastructures: A review. *Compos B Eng.* 2020;189:107892. doi:10.1016/j.compositesb.2020.107892
- 5. Phillips AJ, Cunningham AB, Gerlach R, Hiebert R, Hwang C, Lomans B, Westrich J, Mantilla C, Kirksey J, Esposito R, Spangler L. Fracture Sealing with Microbially-Induced Calcium Carbonate Precipitation: A Field Study. *Environ Sci Technol*. 2016;50(7):4111-4117. doi:10.1021/acs.est.5b05559
- 6. Mujah D, Shahin MA, Cheng L. State-of-the-Art Review of Biocementation by Microbially Induced Calcite Precipitation (MICP) for Soil Stabilization. *Geomicrobiol J.* 2017;34(6):524-537. doi:10.1080/01490451.2016.1225866
- 7. De Muynck W, De Belie N, Verstraete W. Microbial carbonate precipitation in construction materials: A review. *Ecol Eng.* 2010;36(2):118-136. doi:10.1016/j.ecoleng.2009.02.006
- 8. Phillips AJ, Gerlach R, Lauchnor E, Mitchell AC, Cunningham AB, Spangler L. Engineered applications of ureolytic biomineralization: a review. *Biofouling*. 2013;29(6):715-733. doi:10.1080/08927014.2013.796550
- 9. Victoria S. Whiffin. *Microbial CaCO3 Precipitation for the Production of Biocement*. Murdoch University; Doctor of Philosophy (PhD); 2004.
- 10. Cheng L, Cord-Ruwisch R, Shahin MA. Cementation of sand soil by microbially induced calcite precipitation at various degrees of saturation. *Canadian Geotechnical Journal*. 2013;50(1):81-90. doi:10.1139/cgj-2012-0023
- 11. Xiao Y, He X, Zaman M, Ma G, Zhao C. Review of Strength Improvements of Biocemented Soils. *International Journal of Geomechanics*. 2022;22(11). doi:10.1061/(ASCE)GM.1943-5622.0002565
- 12. Whiffin VS, van Paassen LA, Harkes MP. Microbial Carbonate Precipitation as a Soil Improvement Technique. *Geomicrobiol J.* 2007;24(5):417-423. doi:10.1080/01490450701436505
- 13. Achal V, Mukherjee A, Kumari D, Zhang Q. Biomineralization for sustainable construction A review of processes and applications. *Earth Sci Rev.* 2015;148:1-17. doi:10.1016/j.earscirev.2015.05.008
- 14. Rajasekar A, Moy CKS, Wilkinson S. MICP and Advances towards Eco-Friendly and Economical Applications. *IOP Conf Ser Earth Environ Sci.* 2017;78:012016. doi:10.1088/1755-1315/78/1/012016
- 15. Harkes MP, van Paassen LA, Booster JL, Whiffin VS, van Loosdrecht MCM. Fixation and distribution of bacterial activity in sand to induce carbonate precipitation for ground reinforcement. *Ecol Eng.* 2010;36(2):112-117. doi:10.1016/j.ecoleng.2009.01.004
- 16. Avci R. BiyoTrap. Published online 2019.

- 17. Rzhepishevska O, Hakobyan S, Ruhal R, Gautrot J, Barbero D, Ramstedt M. The surface charge of anti-bacterial coatings alters motility and biofilm architecture. *Biomater Sci*. 2013;1(6):589. doi:10.1039/c3bm00197k
- 18. Metwally S, Stachewicz U. Surface potential and charges impact on cell responses on biomaterials interfaces for medical applications. *Materials Science and Engineering: C.* 2019;104:109883. doi:10.1016/j.msec.2019.109883
- 19. Oh JK, Yegin Y, Yang F, Zhang M, Li J, Huang S, Verkhoturov S, Schweikert E, Perez-Lewis K, Scholar E, Taylor T.M, Castillo A, Cisneros-Zevallos L, Min Y & Akbulut M. The influence of surface chemistry on the kinetics and thermodynamics of bacterial adhesion. *Sci Rep.* 2018;8(1):17247. doi:10.1038/s41598-018-35343-1
- 20. Rimola A, Costa D, Sodupe M, Lambert JF, Ugliengo P. Silica Surface Features and Their Role in the Adsorption of Biomolecules: Computational Modeling and Experiments. *Chem Rev.* 2013;113(6):4216-4313. doi:10.1021/cr3003054
- 21. Martin J. Biocorrosion of 1018 Steel in Sulphide Richmarine Environments; a Correlation Between Strain and Corrosion Using Electron Backscatter Diffraction. Published online 2014.
- 22. Aydin ŞÇ. Rapid Detection and Identification of Bacterial Pathogens in Drinking Water Sources Using DNA-Based Methods and Immunoimmobilization Technology. *Bogazici University*, 2007.
- 23. Suo Z, Avci R, Yang X, Pascual DW. Efficient Immobilization and Patterning of Live Bacterial Cells. *Langmuir*. 2008;24(8):4161-4167. doi:10.1021/la7038653
- 24. Suo Z, Yang X, Avci R, Deliorman M, Rugheimer P, Pascual D, Idzerda Y. Antibody Selection for Immobilizing Living Bacteria. *Anal Chem.* 2009;81(18):7571-7578. doi:10.1021/ac9014484
- 25. Yadav AR, Sriram R, Carter JA, Miller BL. Comparative study of solution—phase and vapor—phase deposition of aminosilanes on silicon dioxide surfaces. *Materials Science and Engineering: C.* 2014;35:283-290. doi:10.1016/j.msec.2013.11.017
- 26. Jung D, Biggs H, Erikson J, Ledyard PU. New Colorimetric Reaction for End-Point, Continuous-Flow, and Kinetic Measurement of Urea. *Clin Chem.* 1975;21(8):1136-1140. doi:10.1093/clinchem/21.8.1136
- 27. Herigstad B, Hamilton M, Heersink J. How to optimize the drop plate method for enumerating bacteria. *J Microbiol Methods*. 2001;44(2):121-129. doi:10.1016/S0167-7012(00)00241-4
- 28. Otsu NA. Threshold Selection Method from Gray-Level Histograms. *IEEE Trans Syst Man Cybern* . 1979;9:62-666.
- 29. Deliorman M. The Immunoimmobilization of Living Bacteria on Solid Surfaces and Its Applications. *Montana State University*; 2012.
- 30. Ma L, Pang AP, Luo Y, Lu X, Lin F. Beneficial factors for biomineralization by ureolytic bacterium Sporosarcina pasteurii. *Microb Cell Fact*. 2020;19(1):12. doi:10.1186/s12934-020-1281-z
- 31. Jennings MC, Minbiole KPC, Wuest WM. Quaternary Ammonium Compounds: An Antimicrobial Mainstay and Platform for Innovation to Address Bacterial Resistance. *ACS Infect Dis.* 2015;1(7):288-303. doi:10.1021/acsinfecdis.5b00047
- 32. Berney M, Hammes F, Bosshard F, Weilenmann HU, Egli T. Assessment and Interpretation of Bacterial Viability by Using the LIVE/DEAD BacLight Kit in

- Combination with Flow Cytometry. *Appl Environ Microbiol*. 2007;73(10):3283-3290. doi:10.1128/AEM.02750-06
- 33. Stiefel P, Schmidt-Emrich S, Maniura-Weber K, Ren Q. Critical aspects of using bacterial cell viability assays with the fluorophores SYTO9 and propidium iodide. *BMC Microbiol*. 2015;15(1):36. doi:10.1186/s12866-015-0376-x
- 34. Murata H, Koepsel RR, Matyjaszewski K, Russell AJ. Permanent, non-leaching antibacterial surfaces—2: How high density cationic surfaces kill bacterial cells. *Biomaterials*. 2007;28(32):4870-4879. doi:10.1016/j.biomaterials.2007.06.012
- 35. Nihei T. Antimicrobial Activity of a Novel Silane Coupling Agent Consisting of a Quaternary Ammonium Salt Using a Polymicrobial Biofilm Model. *J Dent Health Oral Disord Ther.* 2017;7(4). doi:10.15406/jdhodt.2017.07.00246
- 36. Bernardi D, DeJong JT, Montoya BM, Martinez BC. Bio-bricks: Biologically cemented sandstone bricks. *Constr Build Mater*. 2014;55:462-469. doi:10.1016/j.conbuildmat.2014.01.019
- 37. Lambert SE, Randall DG. Manufacturing bio-bricks using microbial induced calcium carbonate precipitation and human urine. *Water Res.* 2019;160:158-166. doi:10.1016/j.watres.2019.05.069
- 38. Bu C, Wen K, Liu S, Ogbonnaya U, Li L. Development of bio-cemented constructional materials through microbial induced calcite precipitation. *Mater Struct*. 2018;51(1):30. doi:10.1617/s11527-018-1157-4
- 39. Porter H, Mukherjee A, Tuladhar R, Dhami NK. Life Cycle Assessment of Biocement: An Emerging Sustainable Solution? *Sustainability*. 2021;13(24):13878. doi:10.3390/su132413878

